

**Effects of composition-dependent interatomic interactions on alloying at the Cr/Fe(100) interface**M. Polak,<sup>1,2</sup> C. S. Fadley,<sup>2</sup> and L. Rubinovich<sup>1</sup><sup>1</sup>*Department of Chemistry, Ben-Gurion University of the Negev, Beer-Sheva 84105, Israel*<sup>2</sup>*Materials Science Division, Lawrence Berkeley National Laboratory, Berkeley, California 94720*

(Received 12 August 2001; revised manuscript received 2 January 2002; published 6 May 2002)

Energetic factors that govern intermixing and alloying at the Cr/Fe(100) interface are discussed and applied quantitatively in a model based on locally composition-dependent, surface enhanced Cr-Fe interactions. The calculations, employing the free-energy concentration expansion method without any adjustable energetic parameters, are in good agreement with scanning tunneling microscopy results for Cr growth on Fe(100), as reported previously by Davies *et al.* [Phys. Rev. Lett. **76**, 4175 (1996)]. Following a moderate, mixing related increase in Cr surface fraction, at  $\sim 1$  ML deposited Cr coverage, a sharp transition from a low  $\sim 10\%$  value to  $\sim 30\%$  Cr is predicted. This transition is closely associated with a change of sign in the composition dependent effective pair interactions reported for this system. According to the calculations for deposited coverages  $\geq 2$  ML, a pure Cr layer is separated at the surface, with 1–2 layer sharp interface and slightly Cr-mixed iron layers underneath. At submonolayer Cr deposited coverages only the latter, diffuse part of the interface prevails. Calculated short-range order pair probabilities at the alloy surface and in the bulk agree with experimental values.

DOI: 10.1103/PhysRevB.65.205404

PACS number(s): 68.35.Dv, 68.35.Md, 68.47.De, 05.70.Np

**I. INTRODUCTION**

Properties of thin metal films grown on metal surfaces have drawn considerable interest in recent years. In many systems the interface between substrate and film is not atomically flat, but intermixing and alloy formation occur. Effects of interatomic interactions on metal-metal interfacial phenomena have been extensively studied, mostly for alloys with an ordering tendency.<sup>1</sup> By “ordering” or “mixing” it is meant that *A* atoms in *A-B* alloy tend to be preferentially surrounded by *B* atoms (being the energetically more favorable configuration), as opposed to “demixing” or phase-separation tendency to clustering of like atoms. Somewhat less attention has been paid to alloys and thin films with this tendency for phase separation,<sup>2,3</sup> and to binary systems with concentration-dependent interactions as Fe-Cr (Refs. 4,5) or Fe-Al.<sup>6</sup> The structural origin of magnetic properties related to the topmost deposited layers of Cr on Fe(001) (Refs. 7,8) has been investigated by scanning tunneling microscopy (STM).<sup>9</sup> In contrast to the formation of a chemically abrupt interface, growth at 573 K leads to the formation of a Cr-Fe alloy observed as a distribution of single atomic Cr impurities dispersed in the Fe near-surface substrate for overall coverages under one monolayer (ML). (Only after 2–3 ML Cr deposition does the topmost surface become dominated by Cr.<sup>9</sup>) Monte Carlo simulations with *ab initio* calculated interactions in the dilute limit<sup>10</sup> has confirmed the above and, together with other experimental findings,<sup>11</sup> it has been concluded that Cr-Fe mixing tendency induces strong diffusion of Cr into subsurface Fe layers.

However, with increasing Cr concentration in the alloy the Cr-Fe interaction energetics become even more complex. Thus, diffuse-neutron scattering and resistivity measurements performed on  $\text{Fe}_{1-c}\text{Cr}_c$  alloys, revealed a change of sign of the short-range-order parameters near  $c = 0.1$ .<sup>4,12</sup> The alloys exhibit short-range clustering (demixing of Fe and Cr) at  $c > 0.1$  and a tendency for ordering at  $c < 0.1$ . This inver-

sion of short-range order (and of the pertinent Cr-Fe interactions) was predicted also by generalized perturbation method calculations.<sup>5</sup>

The present work was motivated by the realization that the limit of the low-coverage Cr surface fraction observed on Fe(100) was indeed around  $c = 0.1$ . Therefore, variations of surface and interface layer concentrations with Cr coverage have been evaluated by means of the recently published equilibrium statistical-mechanical “free-energy concentration expansion method” (FCEM),<sup>1,13</sup> while using the above mentioned concentration dependent interactions (including extrapolation to the Fe-rich region). The results are compared with the STM experimental data over a wide range of Cr deposition coverages. A complete theoretical evaluation of the phenomena studied also have to take into account kinetic constraints. However, since the reported experimental data most probably correspond to some steady state conditions, a near-surface “local” equilibrium (including short-range order) within the first several outmost atomic layers was assumed in the FCEM calculations. As is shown, due to the decisive role of the change in sign of the Cr-Fe interactions near Cr concentration  $\sim 0.1$ , such a simplified assumption accounts very well for the experimental data, and provides new insights into this prototypical metal-metal interface problem.

**II. THEORETICAL APPROACH AND ENERGETIC PARAMETERS**

The equilibrium state of alloy surfaces and surface alloys is calculable from the system free energy with pair interaction parameters and entropic contributions.<sup>13</sup> However, since in the present study the interatomic interactions depend on the alloy configuration, some revision of the alloy Hamiltonian and the corresponding free-energy is needed. The formulas we derive are applied to a near-surface alloy thin film

with Cr concentration that depends on the overall Cr deposited coverage.

Using an Ising-like model in which “spin” variables  $\{\sigma_i\}$  describe site occupations, we set  $\sigma_i$  equal to  $1(-1)$  if the site  $i$  is occupied by an  $A(B)$  atom. For the case at hand,  $A = \text{Cr}$  atom and  $B = \text{Fe}$  atom. The alloy configurational energy can then be written as<sup>1</sup>

$$E = \frac{1}{4} \sum_{\{mn\}} (V_{mn}^{AA} + V_{mn}^{BB} + 2V_{mn}^{AB}) + \frac{1}{2} \sum_p \left( \sum_{m \in p \text{ layer}} (\Delta h_p + \Delta H_p^s) \sigma_m \right) + \frac{1}{2} \sum_{\{mn\}} V_{mn} \sigma_m \sigma_n, \quad (1)$$

where  $V_{mn}^{AA}$ ,  $V_{mn}^{BB}$ , and  $V_{mn}^{AB} = V_{mn}^{BA}$  are the interaction energies between the corresponding atoms at site  $m$  and at site  $n$ ,  $\{mn\}$  denotes a pair of lattice sites, and the effective pair interactions read  $V_{mn} = \frac{1}{2}(V_{mn}^{AA} + V_{mn}^{BB} - 2V_{mn}^{AB})$ .

As can be shown,<sup>1</sup>  $\Delta h_p$  and  $\Delta H_p^s$  account for the difference in  $p$ -layer tensions between pure constituents (related to the difference in  $A$ - $A$  and  $B$ - $B$  interaction energies) and for atomic size mismatch (e.g., elastic) energy, respectively. In accordance with the Ising model, these terms, multiplying the “spin” variables, contribute to the “ $p$ -layer fields.”<sup>1</sup>

Substituting  $V_{mn}^{AB} = \frac{1}{2}(V_{mn}^{AA} + V_{mn}^{BB} - 2V_{mn})$ , in Eq. (1) leads to

$$E = \frac{1}{2} \sum_{\{mn\}} (V_{mn}^{AA} + V_{mn}^{BB}) + \frac{1}{2} \sum_p \left( \sum_{m \in p \text{ layer}} (\Delta h_p + \Delta H_p^s) \sigma_m \right) + \frac{1}{2} \sum_{\{mn\}} V_{mn} (\sigma_m \sigma_n - 1). \quad (2)$$

In principle, all three types of interactions ( $V_{mn}^{AA}$ ,  $V_{mn}^{BB}$ , and  $V_{mn}^{AB}$ ) can depend on the alloy concentration, or more specifically, on the *local* average concentration of an atomic cluster, surrounding a pair of lattice sites  $m$  and  $n$ . However, the most important configuration-dependent contribution of interactions, and the one which is responsible for a tendency to order or cluster, is related to the last sum containing  $V_{mn}$ . The first sum does not depend explicitly on the alloy configuration  $\{\sigma_m\}$ , although a weaker dependence on local concentration can exist. Thus, in the present work, we omit the first sum and the following formula for the configuration energy is used as a first attempt to take into account the concentration-dependent order-disorder tendency:

$$E = \frac{1}{2} \sum_p \left( \sum_{m \in p \text{ layer}} (\Delta h_p + \Delta H_p^s) \sigma_m \right) + \frac{1}{2} \sum_{\{mn\}} V_{mn} (\sigma_m \sigma_n - 1). \quad (3)$$

Noting that  $\langle \sigma_m \rangle = 2c_m - 1$ , where  $c_m$  is the site concentration, and that the Bragg-Williams (BW) configurational entropy (for a random alloy) is given by<sup>1</sup>  $S^{\text{BW}} = -k \sum_p N_p [c_p \ln(c_p) + (1 - c_p) \ln(1 - c_p)]$ , the corresponding free energy of an alloy with a set of concentrations  $c_p$  ( $p = 1, 2, \dots$ ) of layers having  $N_p$  sites is in the BW-type approximation

$$F^{\text{BW}'} = kT \sum_p N_p [c_p \ln(c_p) + (1 - c_p) \ln(1 - c_p)] + \frac{1}{2} \sum_p [N_p (\Delta h_p + \Delta H_p^s) (2c_p - 1)] + \frac{1}{2} \sum_{\{mn\}} V_{mn} [(2c_m - 1)(2c_n - 1) - 1]. \quad (4)$$

Contributions of short-range order to the alloy free-energy can be taken into account by means of the approximate FCEM formula<sup>1,13</sup>

$$F = F^{\text{BW}'} + \Delta F^{\text{SRO}} \quad (5)$$

with

$$\Delta F^{\text{SRO}} = -kT \sum_{\{mn\}} c_m (1 - c_m) c_n (1 - c_n) \times \left[ \exp\left(-\frac{2V_{mn}}{kT}\right) + \frac{2V_{mn}}{kT} - 1 \right]. \quad (6)$$

Further, the probability of finding a Cr-Cr pair on the alloy lattice sites  $m$  and  $n$ <sup>13</sup> is given by

$$p_{mn} = c_m c_n - c_m (1 - c_m) c_n (1 - c_n) \left[ 1 - \exp\left(-\frac{2V_{mn}}{kT}\right) \right] \quad (7)$$

which differs from the value  $c_m c_n$ , for the pair probability in a completely random alloy. Correspondingly, the occupation probability of the  $n$  site by a Cr atom under the condition that the  $m$  site is also occupied by a Cr atom is

$$\tilde{p}_{mn} = \frac{p_{mn}}{c_m} = c_n - (1 - c_m) c_n (1 - c_n) \left[ 1 - \exp\left(-\frac{2V_{mn}}{kT}\right) \right]. \quad (8)$$

In order to obtain in-depth layer-by-layer composition profiles of  $N$ -layer surface alloys the free energy (5) was minimized numerically with respect to the layer concentrations, with the constraint of conservation of the overall concentration in the  $N$ -layer film, by making use of the MATLAB computing environment. The alloy model considered here is based on the dependence of interatomic interactions on the local average concentrations ( $\tilde{c}$ ) of chosen clusters surrounding pairs of lattice sites (see the Appendix). Hence, in the process of free energy minimization the direct variation of layer concentrations was accompanied by the resultant variation of the intralayer and interlayer interactions  $V_{pq} = V(\tilde{c}_{pq})$  according to the curve shown in Fig. 1. This curve

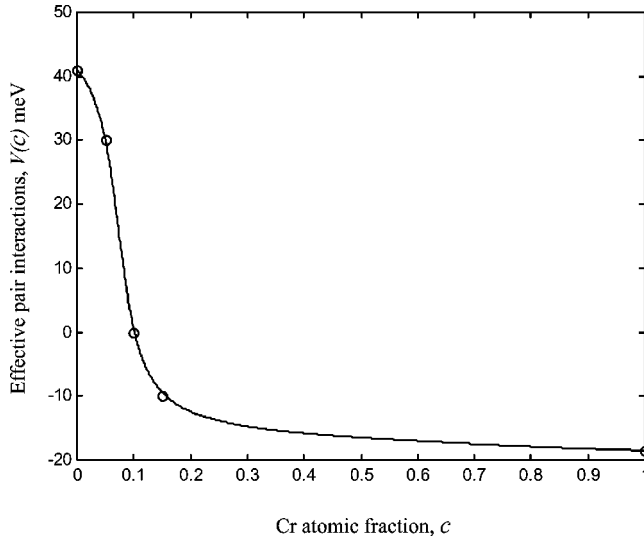


FIG. 1. The dependence of the effective NN and NNN average bulk interactions on the Cr concentration in Cr-Fe alloys. Circles correspond to results of *ab initio* calculations of the effective interactions in the dilute Cr limit (Refs. 10 and 14), diffuse-neutron-scattering measurements (Ref. 4) (for  $c=0.05, 0.1$ , and  $0.15$ ), and the effective interactions estimated from the enthalpy of mixing (Ref. 15) ( $c \approx 1$ ). The line is a mathematical fit to these points.

was obtained by best fits to several data points: the first was obtained from *ab initio* calculations of the interaction strength in the Cr dilute limit,<sup>10,14</sup> the next three were evaluated from diffuse-neutron-scattering measurements,<sup>4</sup> and the last point from the enthalpy of mixing of the Fe rich alloy.<sup>15</sup> These four points were then connected by the smooth curve shown. This curve is thus key to our analysis and it is based on a combination of the best theoretical and experimental data available.

$V_{mn}$  effective interactions both between nearest-neighbor (NN) lattice sites  $V_1$  and between next-nearest-neighbor (NNN) lattice sites  $V_2$  were taken into account in the calculations, and since in the bcc lattice the corresponding distances are rather close, the bulk interactions were assumed to be uniform ( $V=V_1=V_2$ , while more remote bulk interactions were neglected). On the other hand, *ab initio* calculations in the Cr dilute limit revealed considerable enhancement of the effective interaction strength of Fe with Cr impurities on the (100) surface layer of bcc Fe,<sup>10,14</sup> in general agreement with theoretical predictions for transition metal alloys.<sup>16</sup> In particular,  $V=41$  meV, while NN interaction strength at the surface  $V_s=2.54V$  [NN pairs at the (100) surface correspond to the NNN distance in the bulk, Fig. 2] and NNN surface interaction strength,  $V'_s=0.28V$  [(100) surface NNN pairs correspond to the NNNN distance in the bulk]. The  $V_s/V$  and  $V'_s/V$  values, obtained in the Cr dilute limit, were assumed to hold for the entire concentration range.

A very small, several meV, surface-field related contribution  $\Delta h_1 + \Delta H_1^s$  can be estimated either from the calculated segregation energy of Cr ( $-52.8$  meV in the dilute limit<sup>10</sup>) using simple bond-breaking approximation, or directly from surface tension data while neglecting the small size-

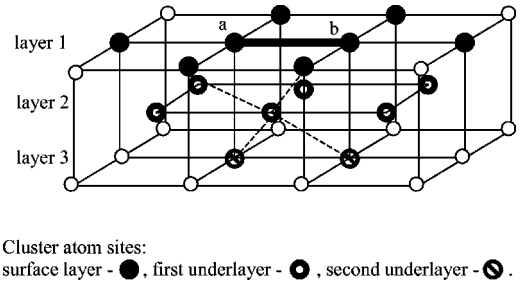


FIG. 2. Near surface bcc(100) cluster that includes a pair of lattice sites [(a) and (b)] and their NN and NNN atoms. NN distances in the bulk are shown by dashed lines; NN distance at the (100) surface (bold line) equals to NNN distance in the bulk.

mismatch ( $\sim 0.6\%$  atomic radius difference) contribution  $\Delta H_1^s$ . Still, in a number of calculations  $\Delta h_1$  was altered in order to examine its possible effects on the calculations. For the second (100) layer the approximation  $\Delta h_2 = \Delta h_1/5$  was used, because it has one broken bond per atom compared to five in the first layer.

### III. RESULTS OF CALCULATIONS

The free energy  $F$ , as given by Eqs. (4)–(6) and evaluated with the above energetic parameters was minimized to give the variation of the Cr fraction in the outermost layer with Cr coverage at a temperature of 573 K and in a case of zero surface field  $\Delta h_1 + \Delta H_1^s \approx 0$  (Fig. 3). Curves are shown for various total numbers of alloy layers being included in the calculation. Within the experimental uncertainties, for Cr

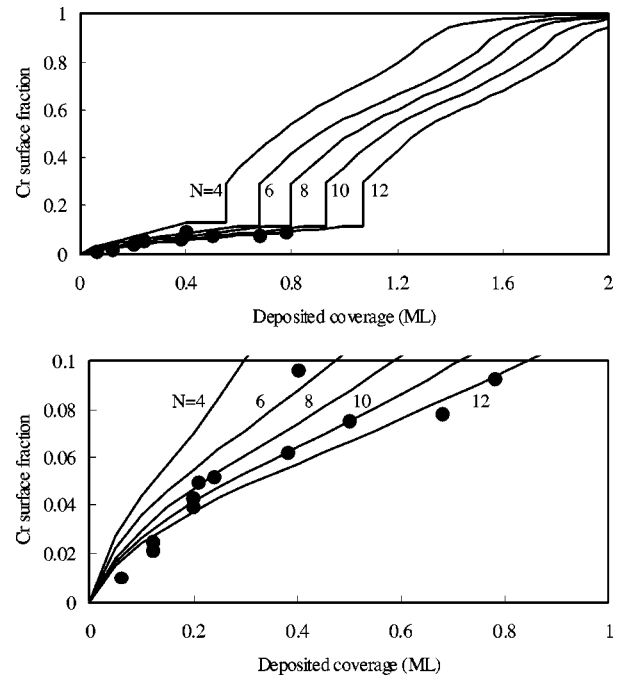


FIG. 3. Calculated variations of Cr fraction in the outermost layer with total deposited Cr coverage for growth on Fe(100) at 573 K in  $N$ -layer surface alloy (100) films with zero surface field and Cr-Fe enhanced surface interactions. Cr concentrations as measured by means of STM are indicated by circles (Ref. 9).

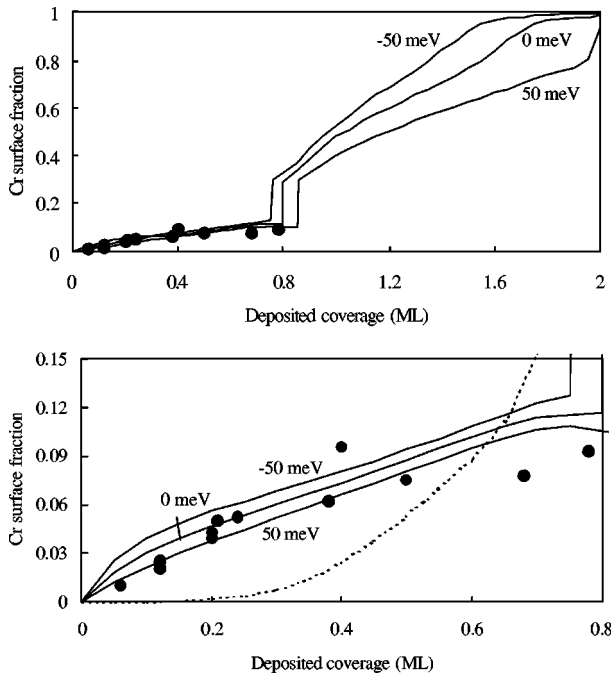


FIG. 4. Variations of Cr fraction in the outermost layer with total deposited Cr coverage for growth at 573 K in eight-layer surface alloy (100) films with different surface fields as indicated near the solid curves. Cr concentrations as measured by means of STM are indicated by circles (Ref. 9). The dotted curve corresponds to calculations that ignore the enhancement in Fe-Cr surface interactions obtained in *ab initio* calculations (Ref. 14).

coverages between  $\sim 0.2$ – $0.6$  the data fit best the curves calculated for  $N=8,10$ , while for higher coverages the  $N=12$  curve fits somewhat better, perhaps due to the longer deposition times resulting in deepening of the interface between the Cr-Fe surface alloy and the pure Fe substrate. Note the generally good agreement with the scanning tunneling microscopy results for these  $N$  values and the fact that no adjustable parameters have been used. Depending on  $N$ , the calculated Cr surface fraction eventually exhibits a sharp rise beyond  $\sim 0.1$ , indicating a surface phase transition. This surface phase transition is clearly associated with the change in sign of the effective pair interaction  $V(c)$  at  $c=0.1$  (see Fig. 1). In particular, when the average concentration (total Cr coverage/ $N$ ) of the near-surface thin-film alloy is  $\leq 0.1$ , the net mixing tendency ( $V_s > V > 0$ ) results in only moderate increase in surface Cr, whereas when coverage/ $N$  is greater than  $\sim 0.1$ , the separation (demixing) tendency ( $V < 0$ ) promotes significant surface segregation. As expected, the onset of this phase transition shifts to higher coverage as the alloy thickness ( $N$ ) increases. It should be further noted that the calculations show that an  $\sim 1$  ML Cr surface fraction is obtained after  $\sim 2$  ML deposited coverage, in agreement with the reported STM data.<sup>9</sup> The dominant role of the interaction strength as compared to the surface-field energetic parameter in this system is demonstrated in Fig. 4. The data seem to fit well the curve corresponding to zero (or very small) surface field, in agreement with theoretical estimates of the latter (see Sec. II). Ignoring the surface NNN interactions had almost no effect on the calculated results, while neglecting the

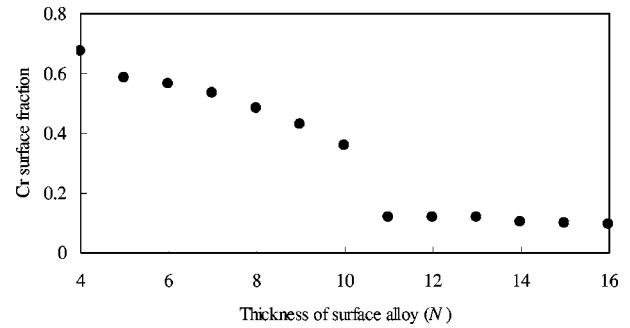


FIG. 5. Calculated Cr fraction in the outermost layer vs assumed thickness of the surface alloy with zero surface field (573 K, 1 ML coverage).

2.54 enhancement factor in the NN surface interactions reduced the calculated low level Cr surface fraction ( $< 0.1$ ) well below the experimental values (Fig. 4, dotted line). This result, related to competition between surface and bulk mixing tendencies, fully justifies the use of the enhanced surface interactions (calculated in the dilute limit<sup>14</sup>), that cause mixing of more Cr solute atoms at the surface layer. Without enhancement, the Cr-Fe mixing tendency in the bulk dominates, whereas for higher Cr fractions ( $> 0.1$ ) the surface and bulk demixing tendencies are compatible, both promoting the above mentioned formation of pure, phase-separated segregating Cr layers. The importance of the interaction dependence on composition is further exemplified in Fig. 5 that shows a transition in the Cr surface fraction around average concentration of 0.1, corresponding to alloy film thickening from  $N=10$  to 11.

In addition to the outermost surface layer composition, the calculations yield layer-by-layer concentrations (Fig. 6). For coverages  $\geq 2$  ML they are characterized by a 1-2 layer thick “primary interface,” between a separated pure Cr layer and slightly Cr mixed iron substrate layers (which might be termed “secondary interface”). For low Cr coverages, such as 0.5 ML, only this mixed interface prevails. The latter is associated with the mixing tendency in the Fe strongly rich alloys ( $V > 0$  for  $c < 0.1$ ), resulting in a somewhat oscillatory profile. The apparent slight increase in Cr concentration calculated for the  $N$ th layer is associated with the arbitrarily chosen pure Fe layer at the  $N+1$  position. According to a

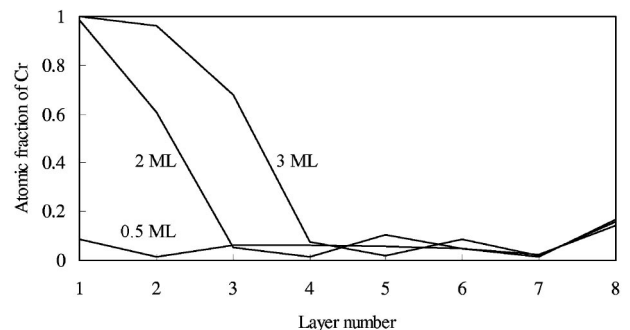


FIG. 6. Calculated depth profiles: Cr layer concentration vs layer number in an eight-layer surface alloy (100) film with zero surface field at 573 K. Coverages are indicated.

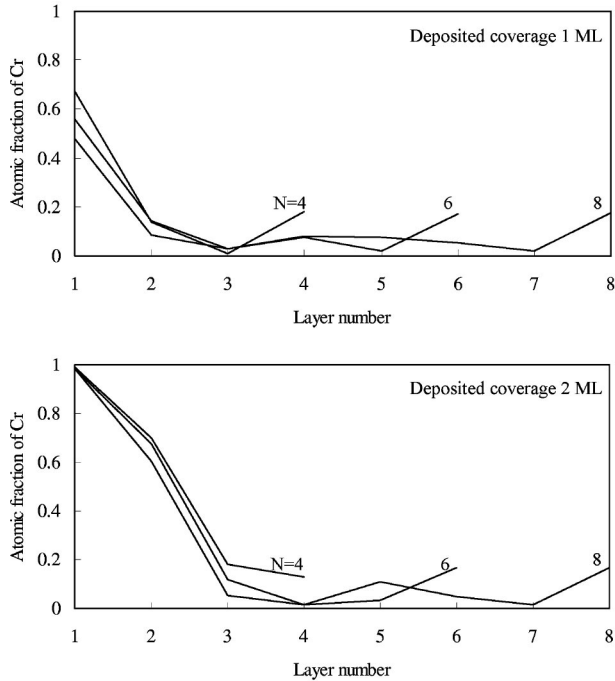


FIG. 7. Cr layer concentration vs layer number in three  $N$  layer surface alloy (100) films (zero surface field, 573 K).

proton and electron-induced AES study,<sup>17</sup> Cr is limited to the two outmost layers for 1 ML coverage, and for 2 ML coverage it is limited to the three outmost layers. These prior results are in general agreement with the above calculated Cr separation/segregation trends, except for the secondary interface. However, AES analysis can not accurately detect small concentrations of mixed Cr in deeper layers as predicted here. Furthermore, the choice of the full alloy film thickness ( $N$ ) does not affect considerably the calculated Cr concentration in the outmost Cr-enriched layers (Fig. 7), except for the Cr surface fraction around the phase transition region (see Fig. 3).

To complement the layer compositional picture, interaction-induced short-range order in this system was estimated by calculating the probability of occupation of Cr neighbor sites by Cr atoms according to Eq. (8). As can be seen from Table I, the theoretical predictions are in good agreement with the STM experimental results obtained in the low-coverage regime.<sup>9</sup> These negative deviations from the random alloy Cr-Cr probability values are in accordance with

TABLE I. Probability of occupation of Cr nearest-neighbor (NN) and next-nearest neighbor (NNN) sites by Cr atoms [Eq. (8)] (for a completely random alloy  $\tilde{p}_{mn}$  equals to the concentration).

| Type | Location | Temperature, K | Effective interaction, meV <sup>a</sup> | Concentration     | FCEM calculations | Experiment          |
|------|----------|----------------|---|-------------------|-------------------|---------------------|
| NN   | Surface  | 563            | $65 \pm 4$                              | $0.059 \pm 0.003$ | $0.010 \pm 0.002$ | $0^b$               |
| NNN  | Surface  | 563            | $7.1 \pm 0.5$                           | $0.059 \pm 0.003$ | $0.046 \pm 0.003$ | $0.038 \pm 0.007^b$ |
| NNN  | Bulk     | 703            | 30                                      | 0.05              | 0.022             | $0.01 \pm 0.02^c$   |

<sup>a</sup>According to the fitted dependence of the bulk effective interactions on Cr concentration (Fig. 1) and the surface-to-bulk interaction ratios (Refs. 10,14).

<sup>b</sup>STM data from Ref. 9.

<sup>c</sup>Recalculated from experimental (Ref. 4) Cowley-Warren SRO parameter.

the Cr-Cr effective repulsion in the alloy (for  $c < 0.1$ ). Still, SRO is quite weak in the low Cr concentration region, where most of the interaction change occurs, as well as for higher Cr contents due to the reduced interaction strength (Fig. 1). Indeed, calculations done within the BW-type approximation [using Eq. (4)] show that compared to SRO effects (calculated by FCEM), the “pure” Cr-Fe energetics (sign and value of  $V$ ) dominate interfacial alloying and phase separation phenomena in this system.

#### IV. SUMMARY

A theoretical approach that takes into account concentration-dependent interatomic interactions at the surface and in the bulk of alloys, as well as short-range compositional order, has been developed as a modification of the statistical mechanical free-energy concentration expansion method (FCEM) and applied to the calculation of the layer-by-layer composition of thin films of binary Cr-Fe alloys on a pure Fe(100) substrate, assuming near-surface local equilibrium.

The calculated variations of Cr fraction in the outermost layer with total deposited Cr coverage are in very good agreement with scanning tunneling microscopy (STM) results.<sup>9</sup> Thus, composition-dependent (and surface enhanced) Cr-Fe interactions lead to a moderate increase in surface Cr at low coverages ( $< 1$  ML) due to mixing with Fe mainly in the underlayers. When its surface fraction (and the average film concentration) exceeds  $\sim 0.1$ , a sharp Cr increase is predicted. This surface phase transition, which marks the onset of almost pure Cr layer segregation at coverages around 2 ML deposited Cr (observed by STM), is attributed to a change in sign of the interaction strength. In this regime the interface between the pure Cr and the mixed substrate underlayers is quite sharp.

This modified FCEM approach is quite general and by utilizing appropriate energetic parameters it can be extended conveniently to unravel layer-by-layer temperature-dependent atomic composition and short-range order in other surface alloys with any lattice structure.

#### ACKNOWLEDGMENTS

M.P. acknowledges the hospitality of C.S.F. during his sabbatical leave at Berkeley.

### APPENDIX: FORMULAS FOR THE AVERAGE CONCENTRATION OF ATOMIC CLUSTERS

Since the local atomic surroundings can affect interactions of a pair of neighboring atoms, an appropriate cluster should be chosen for calculation of its average concentration. In spite of some uncertainty as to its size, inclusion of nearest neighbors (NN) and next nearest neighbors (NNN) seems to be reasonable, considering the fact that first- and second-neighbor distances are very close to each other in the bcc structure. The total number of NN and NNN for every bulk atom is 14. For the (100) layers four of the neighbors are in the same layer, four atoms are in every of the nearest neighbor layers and one atom in every of the next nearest neighbor layers. The local effective interactions  $V_{pq}$  between lattice sites pertaining to (100)  $p$  and  $q$  layers ( $q=p, p\pm 1, p\pm 2$ ) were calculated using average concentrations of clusters, which include a pair of lattice sites and their NN and NNN (Fig. 2).

For near-surface truncated clusters (having missing neighbors) these average concentrations read

$$\tilde{c}_{1,1} = \frac{1}{16}(8c_1 + 6c_2 + 2c_3),$$

$$\tilde{c}_{2,2} = \frac{1}{22}(6c_1 + 8c_2 + 6c_3 + 2c_4),$$

$$\tilde{c}_{1,2} = \frac{1}{17}(6c_1 + 6c_2 + 4c_3 + c_4),$$

$$\tilde{c}_{2,3} = \frac{1}{21}(4c_1 + 6c_2 + 6c_3 + 4c_4 + c_5),$$

$$\tilde{c}_{1,3} = \frac{1}{17}(4c_1 + 4c_2 + 4c_3 + 4c_4 + c_5),$$

$$\tilde{c}_{2,4} = \frac{1}{21}(4c_1 + 4c_2 + 4c_3 + 4c_4 + 4c_5 + c_6),$$

and for  $p > 2$  (nontruncated clusters) the average concentrations are

$$\tilde{c}_{p,p} = \frac{1}{24}(2c_{p-2} + 6c_{p-1} + 8c_p + 6c_{p+1} + 2c_{p+2}),$$

$$\tilde{c}_{p,p+1} = \frac{1}{22}(c_{p-2} + 4c_{p-1} + 6c_p + 6c_{p+1} + 4c_{p+2} + c_{p+3}),$$

$$\begin{aligned} \tilde{c}_{p,p+2} = & \frac{1}{22}(c_{p-2} + 4c_{p-1} + 4c_p + 4c_{p+1} + 4c_{p+2} \\ & + 4c_{p+3} + c_{p+4}). \end{aligned}$$

It can be noted that although the present paper deals with bcc(100) alloys, analogous formulas with somewhat different numerical coefficients can be easily derived for other surface orientations of the bcc lattice, as well as for fcc alloys. In the latter case, only NN sites have to be included in the cluster.

<sup>1</sup>M. Polak and L. Rubinovich, Surf. Sci. Rep. **38/4-5**, 127 (2000).

<sup>2</sup>A.M. Llois and C.R. Mirasso, Phys. Rev. B **41**, 8112 (1990).

<sup>3</sup>S. Delage, B. Legrand, and F. Soisson, Surf. Sci. **377/379**, 551 (1993).

<sup>4</sup>I. Mirebeau, M. Hennon, and G. Parette, Phys. Rev. Lett. **53**, 687 (1984).

<sup>5</sup>M. Hennon, J. Phys. F: Met. Phys. **13**, 2351 (1983).

<sup>6</sup>S. Dorfman, V. Liubich, and D. Fuks, Int. J. Quantum Chem. **75**, 927 (1999).

<sup>7</sup>D.T. Pierce, R.J. Celotta, and J. Unguris, J. Appl. Phys. **73**, 6201 (1993); J. Unguris, R.J. Celotta, and D.T. Pierce, Phys. Rev. Lett. **69**, 1125 (1992).

<sup>8</sup>C. Turtur and G. Bayreuther, Phys. Rev. Lett. **72**, 1557 (1994).

<sup>9</sup>A. Davies, Joseph A. Stroschio, D.T. Pierce, and R.J. Celotta, Phys. Rev. Lett. **76**, 4175 (1996).

<sup>10</sup>L.T. Wille B. Nonas, P.H. Dederichs, and H. Dreyse, Philos. Mag. B **78**, 643 (1998).

<sup>11</sup>B. Heinrich, J.F. Cochran, D. Venus, K. Totland, D. Atlan, S.

Govorkov, and K. Myrtle, J. Appl. Phys. **79**, 4518 (1996).

<sup>12</sup>J.M. Cowley, Phys. Rev. **77**, 669 (1950), defined the Cowley-Warren SRO parameter  $\sigma = (p - c^2)/c(1 - c)$ , related to the probability  $p$  of finding a Cr-Cr nearest neighbor pair. Since  $c^2$  is the pair probability in the completely random state,  $\sigma$  is positive in alloys with tendency to clustering of like atoms, and negative in alloys with ordering tendency.

<sup>13</sup>J.M. Roussel, A. Saul, L. Rubinovich, and M. Polak, J. Phys.: Condens. Matter **11**, 9901 (1999).

<sup>14</sup>B. Nonas, K. Wildberger, R. Zeller, and P.H. Dederichs, Phys. Rev. Lett. **80**, 4574 (1998).

<sup>15</sup>O. Kubaschewski and C. B. Alcock, *Metallurgical Thermochemistry* (Pergamon, Oxford, 1979).

<sup>16</sup>G. Treglia, B. Legrand, and F. Ducastelle, Europhys. Lett. **7**, 575 (1988).

<sup>17</sup>R. Pfandzelter, T. Igel, and H. Winter, Phys. Rev. B **54**, 4496 (1996).